Int J Thermophys
DOI 10.1007/s10765-007-0314-8

Evaluation of Blackbody Cavity Emissivity in the Infrared Using Total Integrated Scatter Measurements

L. M. Hanssen · S. N. Mekhontsev · J. Zeng · A. V. Prokhorov

Abstract Deviations from ideal blackbody (BB) behavior can be characterized by a BB's effective emissivity. The cavity emissivity is most often obtained through a model, given a particular set of input parameters associated with the BB cavity geometry and surface optical properties. It can also be measured directly (radiance) or indirectly (reflectance). A study of BB cavity emissivity using the reflectance method is presented. Several types and designs of blackbody cavities, including those from fixed-point and water bath BBs, using our infrared total integrated scatter (ITIS) instrument for emissivity evaluation are examined. The emissivity is characterized as a function of position on the output aperture, as well as a function of output angle. The measurements have revealed emissivity values, both significantly greater than, and in confirmation of, modeling predictions. For instance, the emissivities of three fixed point BB cavity designs were found to vary significantly despite modeling predictions in the design process of similar behavior. Also, other BB cavities that exhibited poor emissivity performance were re-painted and re-machined, in one case more than once, before the predicted performance was achieved.

Keywords Blackbody · Cavity · Emissivity · Infrared · Radiance temperature · Reflectance

L. M. Hanssen (✉) · S. N. Mekhontsev · J. Zeng
Optical Technology Division, National Institute of Standards and Technology, Gaithersburg, MD 20899, USA
e-mail: hanssen@nist.gov

A. V. Prokhorov
Space Dynamics Laboratory, North Logan, UT 84381, USA

A. V. Prokhorov
Joint NIST/USU Program on Optical Sensor Calibration, Utah State University Research Foundation, North Logan UT, USA

1 Introduction

Two facilities in the Optical Technology Division at the National Institute of Standards and Technology (NIST) provide scales that are referenced to the International Temperature Scale (ITS-90) using blackbody reference sources. These are: (1) the Advanced Infrared Radiometry and Imaging (AIRI) facility for spectral radiance, radiance temperature, and radiance temperature responsivity [1,2]; and (2) the Fourier Transform Infrared Spectrophotometry (FTIS) facility for optical properties of materials including, specifically, spectral emissivity [3]. Both systems rely on blackbody sources as references of spectral radiance. Each system is tied to the ITS-90 through the use of fixed-point sources ranging from Ga at 29.43 °C to Ag at 962 °C. Each makes use of variable temperature blackbodies for obtaining any particular radiance level for comparison with that of blackbodies or samples under test.

For the determination of a blackbody's spectral radiance, together with Planck's law, one requires an object's temperature and spectral emissivity for the given measurement geometry. For the fixed-point blackbodies, the temperature is defined by ITS-90 at the melt/freeze points, which can be unambiguously determined through observation of the melt/freeze plateaux. The only additional information required is the emissivity of the fixed-point cavity, as long as the temperature drop from the solid/liquid interface to the emitting surface is negligibly small, and all ITS-90 requirements such as purity, pressure, isotope content, etc. are met. In addition, the background temperature needs to be determined for the calculation of cavity-reflected radiation (primarily for low temperature and long wavelength situations). For the variable-temperature blackbodies (BB), the spectral radiance is calibrated against the fixed point BBs. This radiance can be assigned to the combination of a temperature and an effective emissivity.

Although additional issues, such as cavity temperature uniformity and the temperature dependence of surface emissivity, need to be considered, much can be learned strictly from ambient temperature reflectance results. Indirect characterization of blackbody cavity emissivity through reflectance measurements has been employed by many investigators over the years [4–8]. We began with measurements using an infrared integrating sphere system developed for the spectral reflectance of materials [9]. Since then, we have built an instrument optimized to accurately measure high-emissivity cavities. The new instrumentation and the results of its use to study a number of fixed-point and variable-temperature blackbody cavities are described in the following sections.

2 Infrared Total Integrated Scatter Instrument Measurements

2.1 Infrared Total Integrated Scatter (ITIS) Instrument

For the determination of cavity emissivity, we use the indirect method of reflectance measurement. By measurement of the directional-hemispherical reflectance, we obtain the directional emissivity, where the angles of reflectance incidence and emissivity are the same. In general, one could use any instrument designed for material diffuse reflectance, including an integrating sphere or conic-mirror device. However,

blackbody cavities have two properties that require special attention in the reflectance measurement: (1) the cavity needs to be measured at normal incidence, since that corresponds to how the cavity will be observed in use—this means that the reflected light, which tends to be concentrated in the direction normal to the cavity aperture, will be retro-reflected toward the open entrance port of the measurement device; and (2) the level of the reflected light is very low. Property (1) means that a typical integrating sphere or collecting mirror, designed for diffuse reflectance measurements of samples, may miss a large fraction of the cavity reflected light, resulting in an incorrect (higher) emissivity value. Property (2) means that a high signal-to-noise ratio is required to distinguish the reflectance from the noise and properly quantify the emissivity for cavity blackbodies.

One solution to accommodate the retro-reflection tendency and low reflectance properties of blackbody cavities is to use laser sources that provide high power and an integrating sphere with a very small entrance port. The use of laser sources can provide sufficient power to use an integrating sphere (which has low throughput) with a small aperture (with a small diameter laser beam), and to underfill small cavity apertures and perform mapping. Such a reflectance instrument employing laser sources and typically used to measure low scatter levels of specular samples such as mirrors or silicon wafers is often called a "Total Integrated Scatter" instrument. This is the approach we have taken. We call our device the ITIS instrument.

A schematic and photo of the ITIS instrument are shown in Fig. 1. The measurement system consists of several infrared lasers (1.32 μm and 10.6 μm used for the results described here) and associated beam shaping optics, polarizing optics, spatial filter, attenuating filters, monitor detector, and chopper. The 200 mm diameter integrating sphere has a 6 mm diameter entrance port for the laser beam, directly opposite the 50.8 mm diameter sample port (which can also hold port reducers as appropriate). The sample cavity is held separate from the integrating sphere on a motorized multi-axis stage, allowing alignment and measurement of the spatial and angular dependence of the reflectance. The sphere position is also controlled for alignment, characterization, and reference measurement. Several detectors, including Ge, MCT, and pyroelectric, are available. The sphere reflectance measurements are performed relative to diffuse and specular gold standards, calibrated at the FTIS facility [9]. All measurement results are for unpolarized light; either the average of data taken with vertical and horizontal polarized input light, or using circularly polarized input light.

The cavity reflectance measurement sequence is shown in Fig. 2a–d. A pair of measurements with a previously calibrated gold standard are first made: (a) of the standard and (b) of the port cover with the same coating as the sphere wall. The ratio of (a) to (b) is used to provide a calibration of the port cover reflectance. The cavity measurement sequence includes (b), (c), and (d). The cavity is measured in (c), then a background measurement of the incident light level, inside the integrating sphere or on the outside of the aperture of the cavity, is made with the remainder of the cavity removed and the beam incident on a distant black surface. For high emissivity cavities, the background may dominate the signal, but the cavity-reflected component can be obtained accurately by maintaining a high degree of stability, not moving the aperture between measurements shown in Fig. 2c, d, and taking into account the minor change in sphere throughput. Finally, in (b) the cavity is retracted slightly and

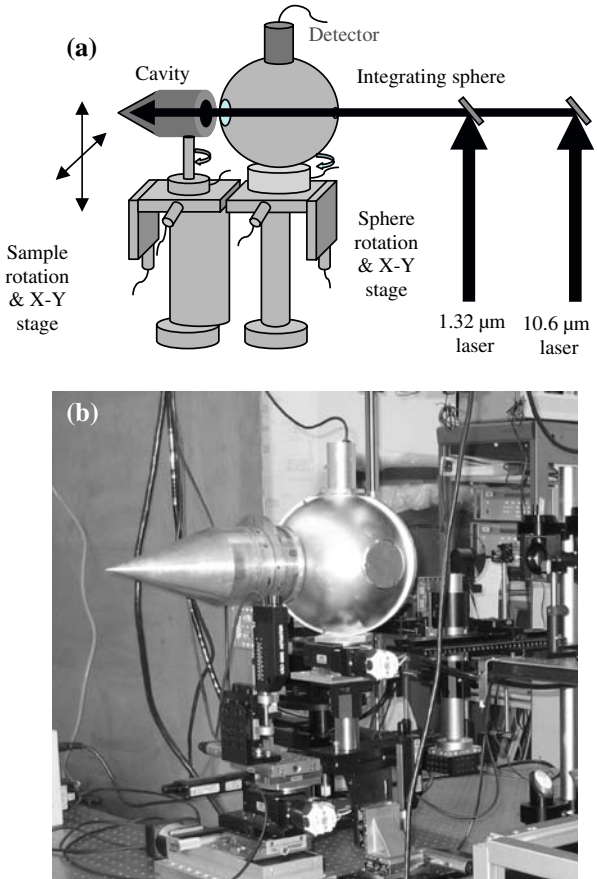

Fig. 1 (**a**) Schematic and (**b**) photo of the infrared total integrated scatter instrument with a water-bath blackbody cavity in the measurement position

the port cover is placed onto the port. There are several ways to perform the reference measurements. For the measurements as described here, we are using a substitution mode. In this case, we separately characterize and correct for the sphere throughput change between measurements.

2.2 Blackbody Cavity Designs

Several fixed-point and variable-temperature blackbody cavity designs are implemented in the NIST AIRI and FTIS facilities. Six cavity designs are investigated in this study: three small graphite cavities with inner diameters of 6 mm–12 mm, and three larger painted copper cavities with inner diameters of 45 mm and 108 mm.

Cross-section schematics of the three graphite fixed-point crucibles are shown in Fig. 3. (The two designs described in [11] are distinct early versions of those shown in Fig. 3b,c. Design (a) is a traditional NIST cavity shape with a 6 mm diameter, a depth of 50.1 mm, and a cone angle of 60° [10]. Designs (b) and (c) are identical

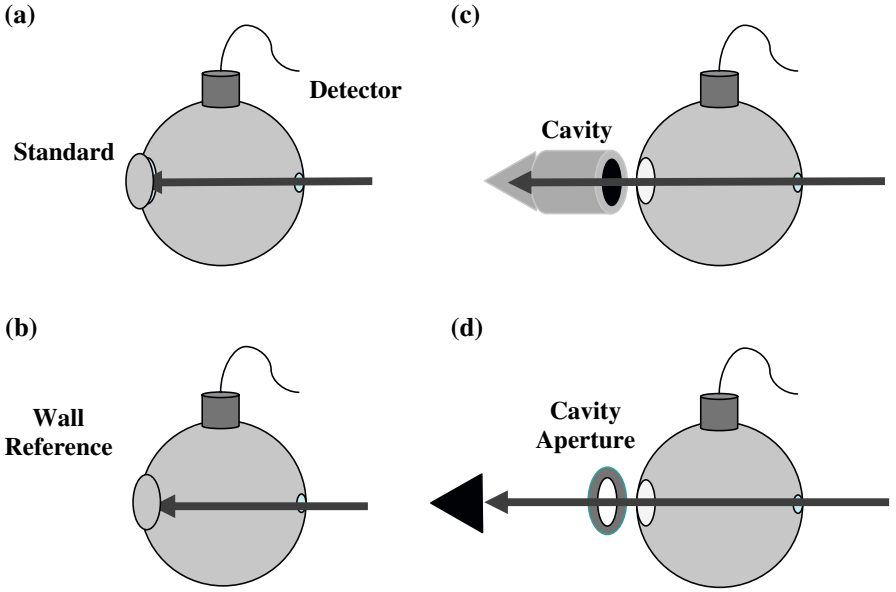

Fig. 2 Sequence of measurements for TIS: (**a**) calibrated standard measurement, (**b**) sphere wall measurement, (**c**) sample cavity measurement, and (**d**) cavity aperture zero measurement

except for the cavity bottom, which are separate parts threaded to mate to the straight cylinder section (this arrangement enables machining of steeper surfaces). Design (b) has a straight cone bottom, with a full angle of 37°. Design (c) has a concentric V-groove bottom, with a groove angle of 37° and a period of 1.5 mm. Multiple copies of the graphite crucibles were manufactured at the same time. One of each type was sacrificed for the reflectance studies. Further details of these fixed-point BBs can be found in [11–13].

Larger cavities and larger apertures are used for the near-ambient temperature range water bath and Ga fixed-point BBs [13]. Both the water bath and initial Ga cavities were two-section cone designs. The Ga cavity shape is shown in Fig. 4a; it has a tapered front section for ease of assembly. The water bath cavity has a very similar shape, but its front section is a straight cylinder; this cavity is used in a new duplicate BB of an existing NIST water bath BB [14]. The Ga cavity is 76 mm in diameter, and 120 mm deep, with a 45 mm diameter aperture. The water bath cavity is 108 mm in diameter and 340 mm deep, with interchangeable apertures ranging down to 25 mm. In addition, the Ga BB incorporates a concentrator (reflector) that is described in a companion paper [13], but was not used in the measurements described here. After the initial ITIS reflectance measurements were performed, the results (described in Section 3) led to a modification of the design: inversion of the cone near its end (at the 6 mm diameter point). This second design as shown in Fig. 4b is currently used for both the new water bath and Ga fixed-point BBs.

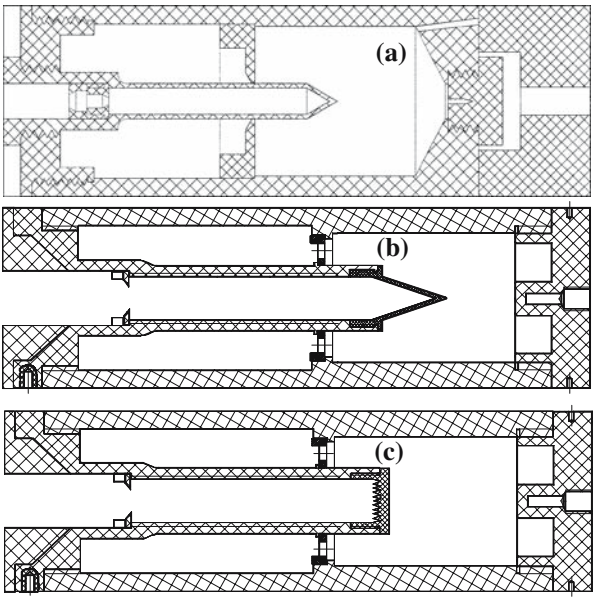

Fig. 3 Designs of three graphite fixed-point blackbody cavities: (**a**) 6 mm diameter small cavity w/60° cone bottom, (**b**) 12 mm diameter cavity w/37° cone bottom, and (**c**) 12 mm diameter cavity w/v-groove bottom

The estimated expanded uncertainty for all reflectance results from the ITIS instruments presented in Section 3, is given by

$$U = \sqrt{(0.15R)^2 + R_0^2} \tag{1}$$

where R is the reflectance value and R_0 is 2×10^{-5} for the 1.32 μm results and 1×10^{-5} for the 10.6 μm results. The first term inside the radical in Eq. 1 is proportional to the measured value, and the second is a constant corresponding to the residual, after background subtraction.

3 Results

3.1 Graphite Fixed-Point Cavities

The effective emissivity of the blackbody cavities is determined by a number of factors including the cavity geometry, the cavity temperature uniformity, and the optical properties of the cavity walls. Knowledge of the reflectance properties of the wall materials is especially critical. In order to help us understand the cavity reflectance measurement results, we also examined the graphite material reflectance properties. We measured both the spectral directional-hemispherical reflectance and single-wavelength bi-directional reflectance distribution function (BRDF) of the graphite flat samples

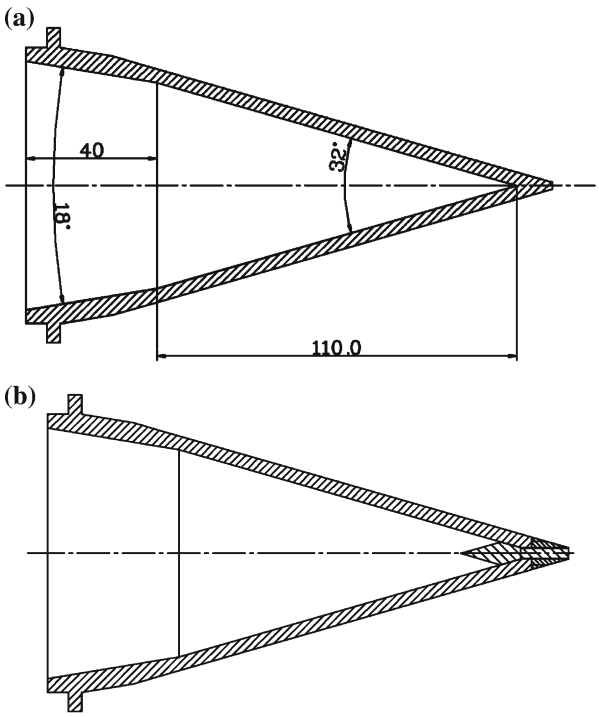

Fig. 4 Designs for three blackbody cavities: (**a**) variable-temperature water-bath cavity and Ga fixed-point cavity with a straight cone bottom and (**b**) Ga fixed-point cavity with a combination straight and inverted cone bottom (dimensions in millimeter)

with varying degrees of surface roughness, and that of a flat surface on the outside of the cavity.

The four samples of graphite, identical to the cavity material in origin and preparation, were measured. Three samples are 38 mm in diameter, as machined ("slightly rough"), partially polished, and roughened with sandpaper. The fourth sample is the flat back-side of the V-groove bottom (15 mm diameter) of one of the cavities. Near-normal (8°) directional-hemispherical reflectance (DHR) spectra of these four samples are shown in Fig. 5, with the cavity sample labeled "glossy" in the figure. The measurements were performed at the FTIS facility [9]. Error bars indicate the expanded ($k = 2$) uncertainties. These results indicate a potential difficulty in predicting the emissivity of a graphite cavity: how do we know the surface finish, and hence its reflectance, of the interior machined surface? At high temperatures, oxidation may take place, causing the formation of particles that may enhance the emissivity as well as alter its specularity [15]. In order to examine the reflectance in more detail, we performed BRDF measurements at 10.6 μm wavelength on all four samples, and at 1.55 μm for the cavity flat sample. BRDF results for the cavity flat sample are shown in Fig. 6: (a) 1.55 μm and (b) 10.6 μm. Note the significant differences between the 1.55 μm and 10.6 μm data. The graphite sample is reasonably diffuse at the short wavelength, but becomes much more specular and has a higher level of reflectance

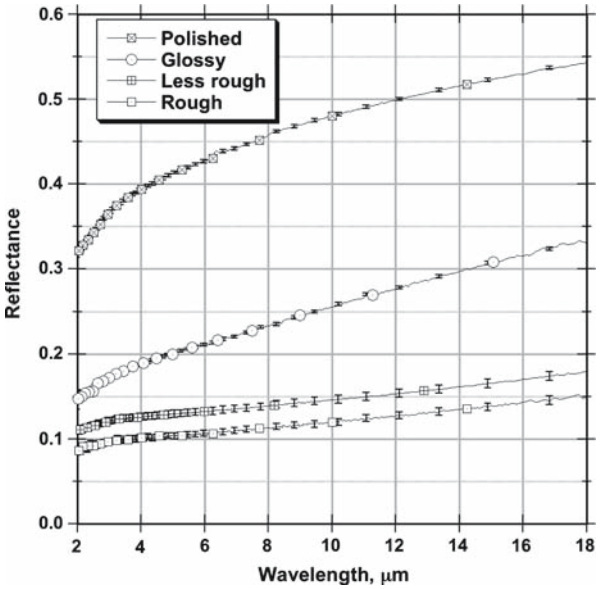

Fig. 5 Reflectance spectra of four graphite samples with varying levels of surface roughness

at the longer infrared wavelength. This difference has a dramatic effect on the cavity emissivity, as we see in the following paragraphs.

The three graphite fixed-point cavities were measured with the ITIS system at both 1.32 μm and 10.6 μm. Four measurements were made, as shown in Fig. 2. In order to properly measure the emissivity of the cavity, the entire cavity must be measured in place, including the section in front of the aperture (the aperture locations in Fig. 3 can be seen, where there is a step reduction of the inner diameter of the cylinder). In operation, this front region is close in temperature to that of the cavity and contributes to the emissivity, while the reflectance is reduced accordingly. At the same time, for the "aperture only" measurement in Fig. 2d, the front section needs to remain in place for proper subtraction. In order to enable both (c) and (d) measurements, we physically separated each cavity just behind the aperture.

The variation in the cavity emissivity across the aperture for the three designs at 1.32 μm is shown in Fig. 7a–c in three-dimensional views, with the reflectance scale shown both in height and gray level. The spot size was approximately 1.5 mm in diameter. In order to highlight the spatial features, the reflectance scale is adjusted for each plot. The plots indicate that the emissivity for the small cavity in (a) has a reflectance value, approximately four times greater than that of the large cavity with the conical bottom in (b). Also, a ringed structure corresponding to the V-grooves in (c) is clearly evident. The ridges and valleys in the reflectance map correspond to the valleys and the ridges, respectively, of the V-grooves. This is because the actual machined surface has a small shallow or flat region at the bottom of the valleys, where the surface is normal to the incident light. Despite this enhanced reflectance structure,

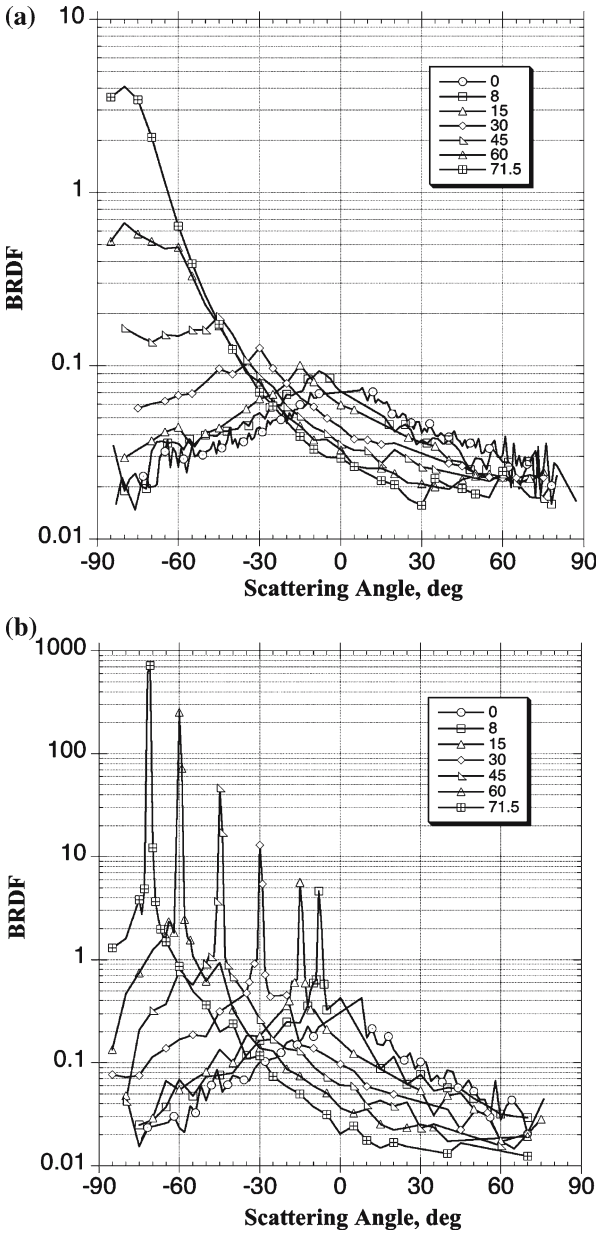

Fig. 6 BRDF of a graphite piece of the cavity (flat back of V-groove bottom section) at (**a**) 1.32 μm and (**b**) 10.6 μm, for different incidence angles. Legend shows the incidence angle, in degrees, onto the sample for each curve. Scattering angle is defined with respect to the normal to the sample. No data are available within 10° of the incidence angle

when averaged over several millimeters, it remains lower than that of the small cavity result.

Similarly, the variation of the cavity emissivity across the aperture for the three designs at a much longer wavelength of 10.6 μm is shown in Fig. 8a–c. The spot size used was also approximately 1.5 mm in diameter. The reflectance levels of all the cavities are significantly greater than at 1.32 μm. This qualitative behavior is to be expected, given the higher reflectance levels for 10.6 μm input, seen in Figs. 5 and 6. Both (a) the small cavity and (b) the large cavity with the conical bottom have reflectance levels approximately four times that measured at 1.32 μm. In contrast, the reflectance of the V-groove cavity has increased by an order of magnitude. Structures in the map associated with the groove locations exist, but are very shallow. We believe that the combination of the increased specular nature of the reflectance of the graphite at 10.6 μm and the non-ideal flat regions in the V-groove valleys, which will retro-reflect any specular portion of the input light, leads to this large reflectance increase.

We also measured the angular dependence of the cavity emissivity to be able to predict the performance for pyrometers with differing fields of view or f/#. The results are shown in Fig. 9. The angular variation is related to the spatial variation, since the input spot moves across the cavity bottom with change of incidence angle, but the change in angle also means that specularly reflected components of the light will be directed to different locations within the cavity, resulting in additional angular variability. The plot of angular variation in Fig. 9a,b exhibit the same relative reflectance as seen in the spatial maps of Figs. 7 and 8. A careful examination of the V-groove curves reveals a correspondence between the peaks of maximum reflectance in (a) and the less distinct relative maxima in (b). The more uniform higher level of reflectance in (b) is consistent with the BDRF measurements shown in Fig. 6b that indicate a significantly greater reflectance for the incidence angle on the cone (71.5°) than in (a).

3.2 Water Bath and Ga Fixed-Point Cavities

We examined two similar cavities used for our variable-temperature water-bath blackbody and our Ga fixed-point blackbody. All measurements were made at 10.6 μm. The cavities were made of copper and painted with specular black paints: Testors black for the water bath blackbody cavity and Aeroglaze Z-302 for the Ga fixed-point blackbody cavity [16]. ITIS measurements were an integral part of the construction of the blackbodies. Measurements were made shortly after the initial coatings of the cavities. Based on the results, the initial cavity designs shown in Fig. 4a were altered to improve the emissivity by insertion of a small inverted cone, as shown in Fig. 4b.

The spatial variation of the initial water-bath blackbody cavity reflectance is shown in Fig. 10. The emissivity at the center of the cavity has a strong maximum, contrary to what calculations for a straightforward cone predict. The 1.2×10^{-3} reflectance maximum indicates the existence of a small flat region, due to either the base cone termination or a paint meniscus, which enhances the reflectance in the center. The higher-reflectance region is defined by the larger of the cavity flat or the beam width (in this case, the beam half-width is about 1.5 mm). Outside the center, the reflectance level is about a decade lower.

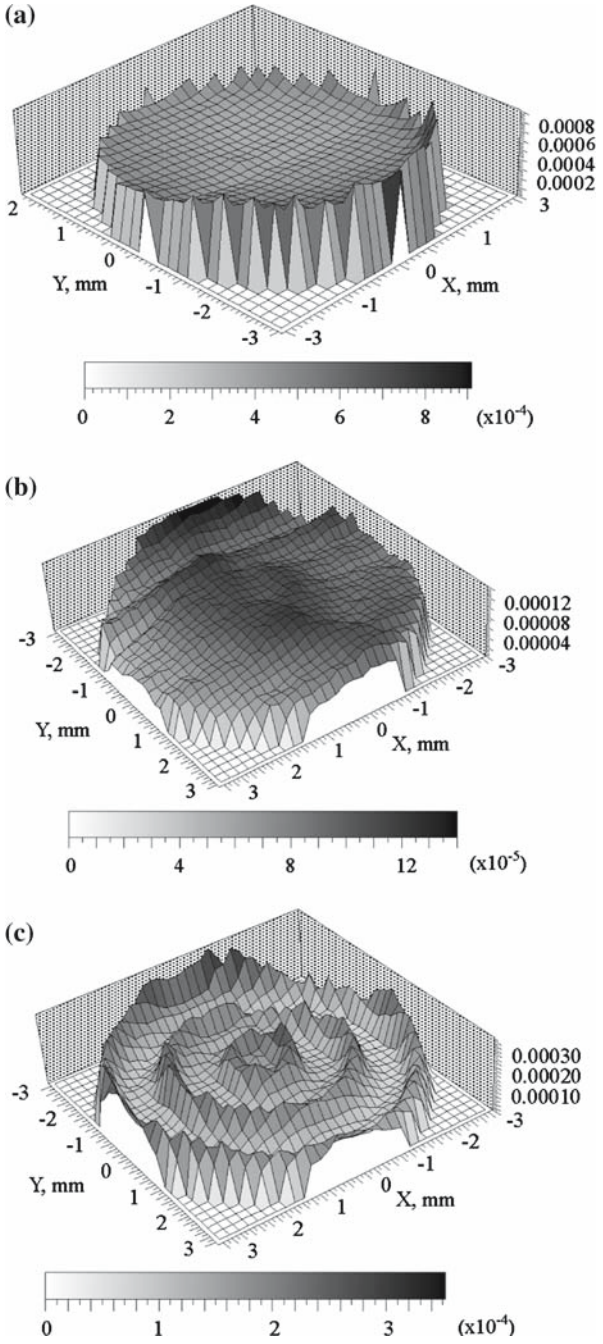

Fig. 7 Effective emissivity scan of graphite fixed-point cavities at 1.32 μm: comparison of three designs: (**a**) small cone cavity, (**b**) large cone cavity, and (**c**) large V-groove cavity

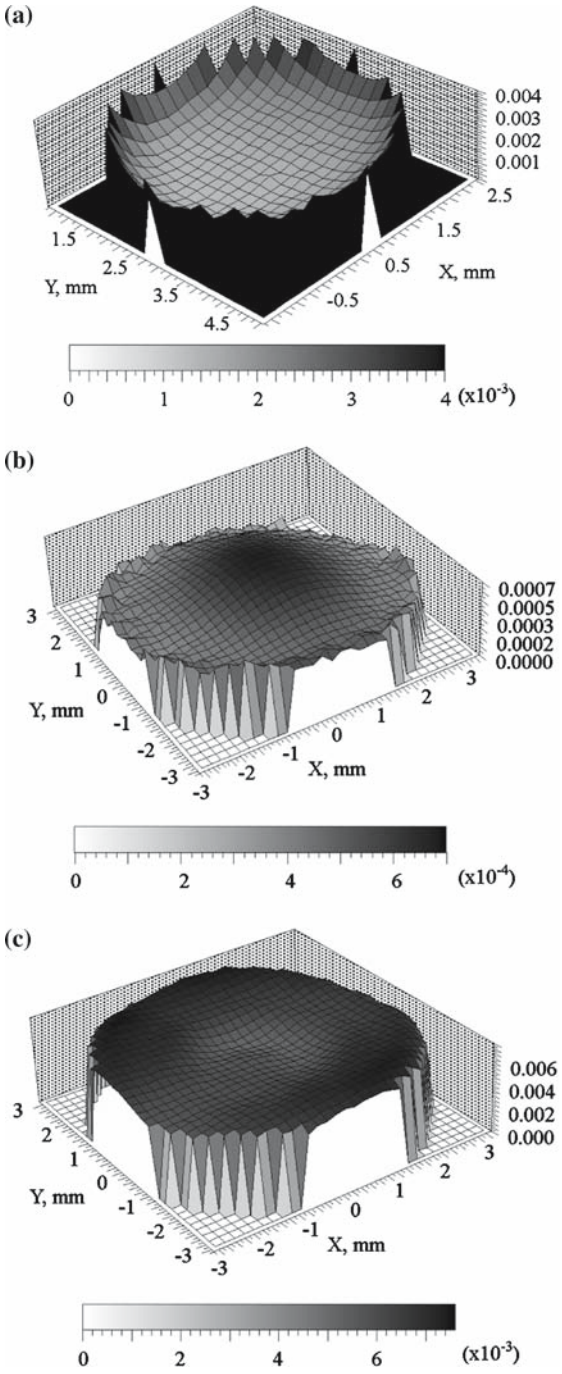

Fig. 8 Effective emissivity scan of graphite fixed-point cavities at 10.6 μm: comparison of three designs: (**a**) small cone cavity, (**b**) large cone cavity, and (**c**) large V-groove cavity

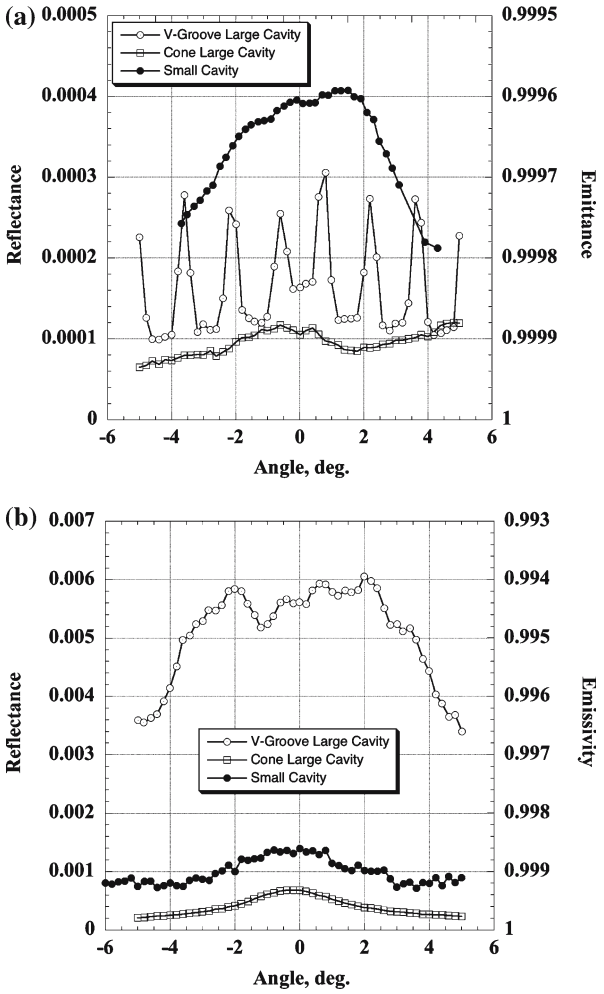

Fig. 9 Angular dependence of effective emissivity of graphite cavities at (**a**) 1.32 μm and (**b**) 10.6 μm

After these results were obtained, the cone was modified to include an inverted cone section in the center, as described in [13]. The reflectance map of the modified cavity is shown in Fig. 11a. The central maximum has disappeared and the reflectance maximum reduced by a factor of 3. The remaining structure appears as a ring with a diameter of about 16 mm and a maximum in the map section highlighted as (b). This structure is likely due to an imperfection in the machined cone, which occurred when the work was interrupted for a period of time. An examination of another reflectance map performed on the initial straight cone cavity is shown in Fig. 11c, with an expanded scale that reveals the same structure at approximately the same reflectance level. (This structure does not appear in Fig. 10, because it is located below the scanned region.)

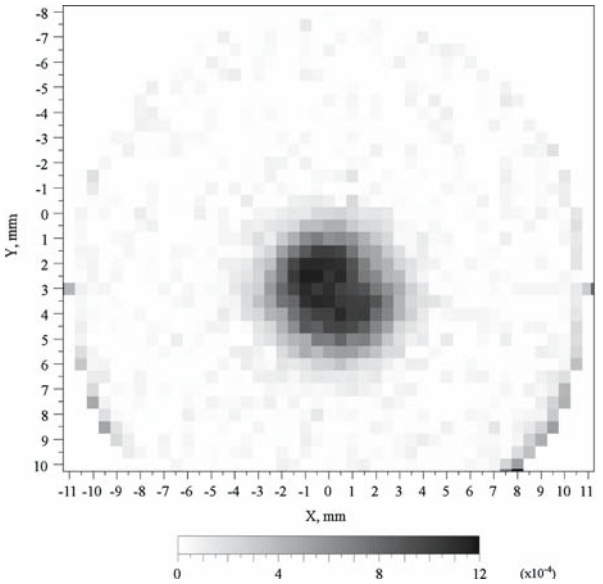

Fig. 10 Effective emissivity of cone cavity for water-bath blackbody: initial coating

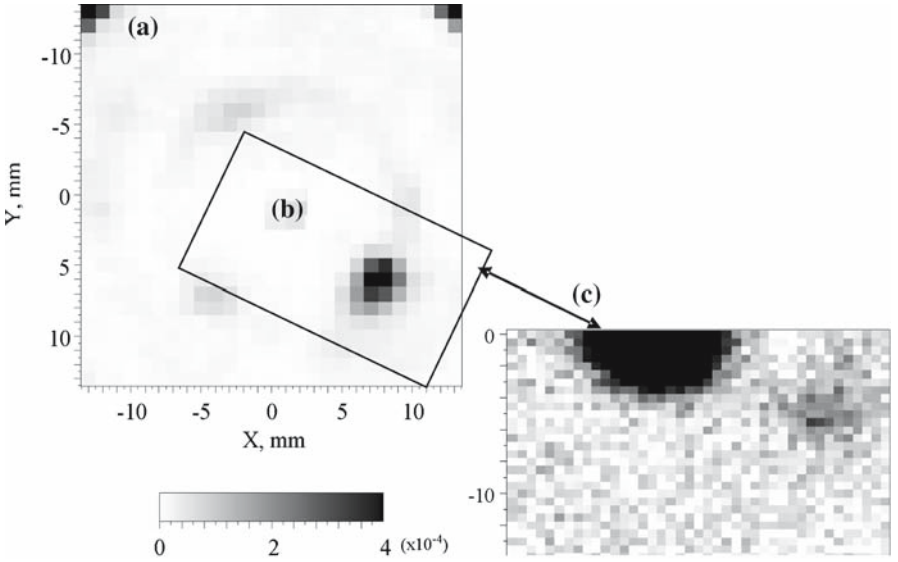

Fig. 11 Effective emissivity of cone cavity for water-bath blackbody: (**a**) inverted cone apex with recoat, (**b**) region with prominent feature, and (**c**) initial coating (expanded scale)

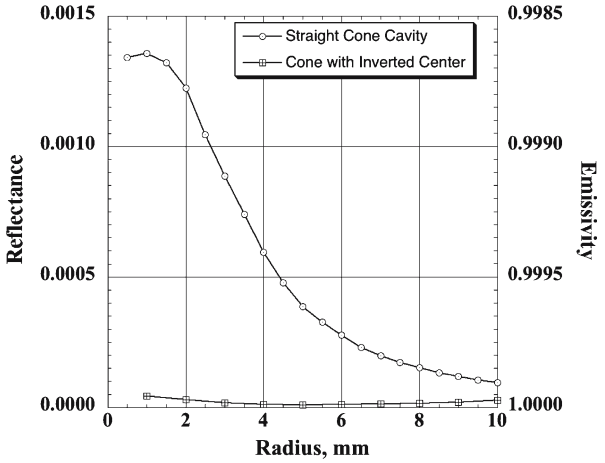

Fig. 12 Effective emissivity of cone cavity for water bath blackbody as a function of size of viewed region

The spatial and angular variation of reflectance results can be integrated to determine an effective emissivity for the cavity when viewed by a pyrometer with a specific viewed spot size and field-of-view. The effective reflectance/emissivity versus viewed spot radius for the water-bath blackbody is shown in Fig. 12, as calculated from cavity spatial map data of Figs. 10 and 11. The results again show the significant improvement in reflectance achieved by the addition of the inverted cone section. The other important fact to note is that the emissivity changes significantly with spot radius. For example, for the straight cone cavity, a pyrometer designed with a large (20 mm diameter) spot size would see an emissivity of 0.9999, whereas one with a small (4 mm diameter) spot size would see an emissivity of only 0.9988. In addition, the small spot pyrometer measurement would be very sensitive to alignment.

The Ga fixed-point cavity similarly was initially made with a straight cone. A map of its spatial variation of reflectance was very similar to the water-bath blackbody cavity (Fig. 11) with a maximum reflectance of 8×10^{-4}. The cavity was stripped and repainted. Unfortunately, the maximum reflectance increased to 1.5×10^{-3}, with the resulting map shown in Fig. 13a (Fig. 13a–c shown on the same scale for comparison purposes). Next, the cavity was modified with a center inverted cone section as shown in Fig. 4b. The subsequent map again showed an improved (lower) reflectance level as seen in Fig. 13b. No significant structure was seen at the inverted cone. At a later time, after the blackbody was assembled and placed into operation, the cavity was removed and re-measured. The resulting reflectance map is shown in Fig. 13c. Much of the map duplicates the earlier result of (b). However, additional increased reflectance (3×10^{-4}) spots, located where the straight and inverted cones meet, appeared. Most likely these spots are due to some small regions of paint that separated from the copper around or near the mating threads. The cavity reflectance remains significantly lower than for the original straight cone and satisfactory for operation of the blackbody as demonstrated in [13]. Nevertheless, we anticipate recoating the cavity in the near future.

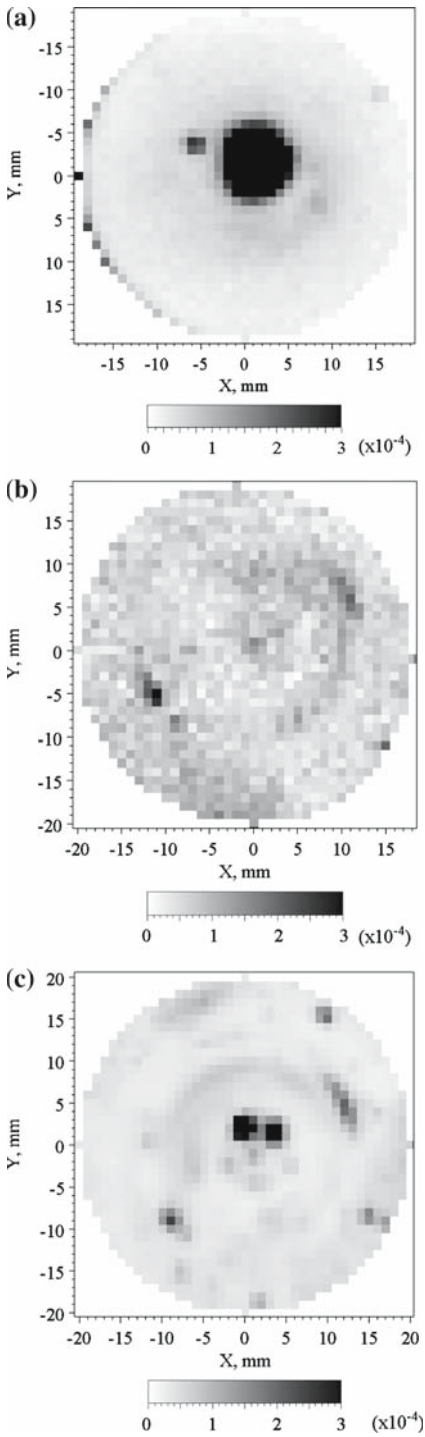

Fig. 13 Effective emissivity of cavity for Ga fixed point blackbody with inverted apex; (**a**) scan of initial simple cavity, (**b**) scan of inverted cone modified cavity, and (**c**) scan of cavity installed into blackbody after operation and temperature cycling

4 Discussion and Conclusions

Discrepancies between emissivity modeling and measurement can exist because the performance of blackbody cavities is dependent on the details and quality of the manufacture (machining, painting, etc.), on the actual coating reflectance and BRDF, and on the degree to which the model can match the actual cavity parameters. A modeled emissivity value can be used with confidence only if the cavity is demonstrated to be manufactured to an appropriate set of specifications and that the cavity does not deviate from the assumptions made in the model. Otherwise, a prudent course is validation via direct measurement of the blackbody performance.

We have found the careful measurement of the reflectance properties of our blackbody cavities at room temperature using the ITIS system to be a valuable tool for the evaluation of blackbody emissivity. ITIS measurements of our blackbody cavities have been critical to the selection and improvement of all blackbodies for which we have made reflectance measurements. The large cone cavity design was selected as the best for use in our graphite fixed-point blackbodies out of the three designs available. The reflectance data enabled us to improve the emissivity performance of both our variable-temperature water-bath blackbody and our Ga fixed-point blackbody, and alert us to a potential problem with the improved design.

The results obtained are complementary to those from other tools available, including Monte Carlo ray-trace modeling, finite-element thermal modeling analysis, and direct spectral radiance measurement comparisons with other well-characterized blackbodies [17,1]. Experimentally determined values for emissivity, using both direct and indirect methods, enable us to avoid the use of incorrect emissivity values, resulting from approximations and perhaps incorrect assumptions about the cavity coating properties and exact cavity geometry. Modeling can then be used to help understand the origin of the emissivity values and whatever structure might be observed. In addition, modeling can be used to deal with temperature non-uniformities in the cavities. It is important to remember that the emissivity obtained from indirect reflectance measurements is only valid for an isothermal cavity. If the cavity has sections at different temperatures, then one requires additional information, such as from appropriate modeling, to obtain the correct emissivity.

We plan to pursue complete characterization of the materials used (including full BRDF and angle-dependent DHR), make the Monte Carlo models more accurate (incorporating the measured BRDF and DHR), and achieve agreement between the measured and calculated emissivities for validation of our uncertainties.

References

1. S.N. Mekhontsev, V.B. Khromchenko, L.M. Hanssen, NIST Radiance Temperature and Infrared Spectral Radiance Scales at Near-ambient Temperatures. in *Proceedings of TEMPMEKO 2007* (to be published in Int. J. Thermophys.)
2. J. Envall, S.N. Mekhontsev, Y. Zong, L.M. Hanssen, Spatial Scatter Effects in the Calibration of IR Pyrometers and Imagers. in *Proceedings of TEMPMEKO 2007* (to be published in Int. J. Thermophys.)
3. L.M. Hanssen, S.N. Mekhontsev, V.B. Khromchenko, Proc. SPIE **5405**, 1 (2004)
4. F.J. Kelly, D.G. Moore, Appl. Optics **4**, 31 (1965)
5. R.P. Heinisch, R.N. Schmidt, Appl. Optics **9**, 1920 (1970)

6. O.C. Jones, C. Forno, Appl. Optics **10**, 2644 (1971)
7. F. Sakuma, L. Ma, in *Proceedings of TEMPMEKO 2004, 9th International Symposium on Temperature and Thermal Measurements in Industry and Science*, ed. by D. Zvizdić, L.G. Bermanec, T. Veliki, T. Stašić (FSB/LPM, Zagreb, Croatia, 2005), pp. 563–568
8. S. Galal Yousef, P. Sperfeld, J. Mettzdorf, Metrologia **37**, 365 (2000)
9. L.M. Hanssen, S.G. Kaplan, Anal. Chim. Acta **380**, 289 (1998)
10. R.D. Lee, Metrologia **2**, 150 (1966)
11. S.N. Mekhontsev, V.B. Khromchenko, A.V. Prokhorov, L.M. Hanssen, in *Proceedings of TEMPMEKO 2004, 9th International Symposium on Temperature and Thermal Measurements in Industry and Science*, ed. by D. Zvizdić, L.G. Bermanec, T. Veliki, T. Stašić (FSB/LPM, Zagreb, Croatia, 2004), pp. 581–586
12. K.D. Mielenz, R.D. Saunders, J. Shumaker, J. Res. Natl. Inst. Stand. Technol. **95**, 49 (1990)
13. V.B. Khromchenko, S.N. Mekhontsev, L.M. Hanssen, Design and Evaluation of Large Aperture Gallium Fixed Point Blackbody. in *Proceedings of TEMPMEKO 2007* (to be published in Int. J. Thermophys.)
14. J.B. Fowler, J. Res. NIST **100**, 591 (1995)
15. For example, we received a separate V-groove sample from the graphite manufacturer. Initial spectral reflectance measurements resulted in greater than expected emissivity (lower reflectance) than calculations predicted (by a factor of 3) [13]. Some time later, air was blown over the sample to remove a piece of lint. It was observed that the sample had been covered by graphite "dust" which was blown off. A second reflectance measurement resulted in values closer to the expected results
16. Certain commercial equipment, instruments, or materials are identified in this paper for information only. Such identification does not imply recommendation or endorsement by the National Institute of Standards and Technology
17. A.V. Prokhorov, S.N. Mekhontsev, L.M. Hanssen, Radiative Properties of Blackbody Calibration Sources: Recent Advances in Computer Modeling. in *Proceedings of TEMPMEKO 2007, Int. J. Thermophys.*, DOI: 10.1007/s10765-007-0285-9